Available online at www.sciencedirect.com

ScienceDirect

Scripta Materialia 102 (2015) 83–86

Scripta MATERIALIA

www.elsevier.com/locate/scriptamat

On the relation between orientation relationships predicted by the phenomenological theory and internal twins in plate martensite

Loïc Malet* and Stéphane Godet

4MAT, Université Libre de Bruxelles, Brussels, Belgium

Received 22 December 2014; revised 12 February 2015; accepted 13 February 2015
Available online 3 March 2015

The phenomenological theory of martensite crystallography predicts two equivalent solutions for a particular habit plane in the case of a Fe–Ni–C alloy. Those two solutions differ in the magnitude of the inhomogeneous shear and in the orientation relationship (OR) they hold with austenite. Only the OR associated to the low shear solution has been observed experimentally so far. In the present study, the orientation relationship associated to the high shear solution is assessed experimentally using TEM measurements.

Keywords: Martensite; Crystallography; Twinning; ACOM TEM; Orientation relationship

The major characteristic feature of the substructure of lens martensite forming in high carbon steels or in Fe-High Ni alloys is its internal twinning [1–3]. The amount of internal twinning is known to depend on the transformation temperature in Fe-High Ni alloys [4,5]. In martensite forming at relatively high temperatures, internal twinning is confined in a narrow band known as the midrib. In martensite forming at the lowest temperatures (below about −120 °C in Fe–Ni–C alloys [5]), internal twins extend over the entire thickness of the plate. The presence of such internal defects has commonly been related in the literature to the lattice invariant shear (LIS) hypothesized in the phenomenological theory of martensite crystallography (PTMC) to convert the Bain strain into an invariant plane strain [6]. More precisely, if the LIS system is chosen to be $(1\,0\,1)_\gamma[1\,0\,\bar{1}]_\gamma$, the theory predicts two equivalent possibilities for each habit plane solution. Those two possibilities come from two distinct Bain distortions (whose compressions axis are mirrors of each other through the plane of the LIS) and differ in the magnitude of the LIS. They are referred to as the low and high shear solutions [6,7]. Those two equivalent transformation paths could in principle be distinguished through the orientation relationship they hold with the austenite [8]. In this framework, an internally twinned martensite plate is seen as an alternate stacking of those two orientations referred to as the matrix (low shear solution) and the twin (high shear solution). Those two solutions are formally equivalent and could in principle be formed experimentally. Interestingly, the low shear solution is always produced in preference to the high shear one. Bowles and Mackenzie consequently supposed that the twin orientation was less favoured because of the larger magnitude of the LIS involved in its formation [7]. This preponderance of the low shear orientation may also explain why a single orientation relationship has systematically been reported for lens martensite forming in Fe-High Ni alloys [6,9]. This experimental OR is indeed quite close to the OR predicted by the theory in the low shear case and is located between the Nishiyama–Wassermann (N–W) OR ($\{1\,1\,1\}_\gamma||\{0\,1\,1\}_\alpha, \langle\bar{1}\,1\,2\rangle_\gamma||\langle 0\,\bar{1}\,1\rangle_\alpha$) and the Kurdjumov–Sachs (KS) OR ($\{1\,1\,1\}_\gamma||\{0\,1\,1\}_\alpha, \langle\bar{1}\,0\,1\rangle_\gamma||\langle\bar{1}\,\bar{1}\,1\rangle_\alpha$) [7]. More recent EBSD studies by Shibata et al. have revealed an orientation spread inside lenticular martensite in Fe-High Ni alloys [10,11]. The densely twinned midrib region holds an orientation relationship close to the Greninger–Troiano (GT) OR ($\{1\,1\,1\}_\gamma$ 1° from $\{0\,1\,1\}_\alpha, \langle\bar{1}\,0\,1\rangle_\gamma$ 2.5° from $\langle\bar{1}\,\bar{1}\,1\rangle_\alpha$) while the untwined region close to the austenite/martensite interface holds a near K–S OR. Though measurable, the orientation spread measured in lens martensite is small and continuous (about 3°). Furthermore, it was not possible for those authors to index the twin orientation near the midrib. As a consequence, it was not possible for them to measure directly the OR between the twin orientation and the austenite. This may be attributed to the large interaction volume of the SEM-based diffraction techniques (a few 1000 nm^3 at usual acceleration voltages i.e. 15–20 kV) that encompass both the twin and its matrix orientations. Since the volume fraction of the twin orientation is smaller, the resulting Kikuchi pattern is representative of the matrix orientation only. TEM-based diffraction techniques seem therefore more appropriate to study the OR of lens martensite. In a recent TEM analysis of lens martensite, Stormwinter et al. were indeed able to index separately the

* Corresponding author.

http://dx.doi.org/10.1016/j.scriptamat.2015.02.019
1359-6462/

twin and matrix orientations of a martensite plate formed in Fe–1.2C by means of automated crystal orientation measurements (ACOM) [12]. Unfortunately, since no retained austenite was present in the scanned area, those authors were not able to measure the OR between those two orientations and the parent austenite. Hence, the OR associated with the high shear solution has not been measured experimentally yet.

In what follows, the phenomenological theory of martensite is applied for the case of a Fe–30.5Ni–0.155C alloy following the derivation and notations used in [13,14]. The two ORs predicted by the theory are expressed in terms of parallelism conditions between close-packed planes and directions in both phases. The relevance of those predictions is tested against TEM measurements performed on a twinned martensite plate.

The lattice parameters of Fe–30.5%Ni–0.155C determined by X-ray diffraction are $a_\gamma = 0.3591$ nm and $a_\alpha = 0.2875$ nm for austenite and martensite, respectively. The Bain strain matrix in the standard reference frame of austenite reads:

$$\boldsymbol{\gamma B \gamma} = \begin{bmatrix} 1.1322 & & \\ & 1.1322 & \\ & & 0.8006 \end{bmatrix} \tag{1}$$

The lattice invariant shear (LIS) is assumed to be a simple shear on the $\{1\,1\,2\}_\alpha$ plane in the $\langle 1\,1\,1\rangle_\alpha$ direction in martensite. For the present example, the specific variant $(1\,1\,2)_\alpha[1\,1\,\bar{1}]_\alpha$ is selected and the following variant of the correspondence matrix is chosen:

$$\boldsymbol{\alpha C \gamma} = \begin{bmatrix} 1 & -1 & 0 \\ 1 & 1 & 0 \\ 0 & 0 & 1 \end{bmatrix} \tag{2}$$

By making use of this correspondence matrix, the present variant of the shear system can be expressed in the reference frame of austenite as $(1\,0\,1)_\gamma[1\,0\,\bar{1}]_\gamma$. The first step in the calculation is to find the line and the plane normal that are left undistorted, though rotated, by the Bain strain. Once defined, those unextended lines and normal will be used to find the rigid body rotation ($\boldsymbol{\gamma R \gamma}$) that allows the Bain strain to be converted into an invariant-line strain ($\boldsymbol{\gamma S \gamma}$). If the undistorted line is chosen to be a normalized vector, lying in the $(1\,0\,1)_\gamma$ plane, which is undistorted by the Bain strain, then its components have to satisfy three equations describing the fact that it lies respectively on a unit sphere, a plane and an ellipsoid [13,14]. When solved simultaneously, those three equations give two solutions for the undistorted line:

$$\boldsymbol{u} = [0.6632\,0.3467\,\overline{0.6632}]_\gamma,\ \boldsymbol{v} = [\overline{0.6632}\,0.3467\,0.6632]_\gamma \tag{3}$$

In the same manner, if the undistorted normal is chosen to be a normalized vector, defining a plane containing the $[1\,0\,\bar{1}]_\gamma$ direction, which is undistorted by the Bain strain, then its components have to satisfy three equations. When solved simultaneously, those three equations give two solutions for the undistorted normal:

$$\boldsymbol{h} = [0.5310\,0.6603\,0.5310]_\gamma,\ \boldsymbol{k} = [0.5310\,\overline{0.6603}\,0.5310]_\gamma \tag{4}$$

We have now to find the rigid body rotation which brings the undistorted line and the undistorted normal back to their original positions so as to make them an invariant line and an invariant normal, respectively. However, we have found that there are two undistorted lines and two undistorted normals. There are consequently four ways of choosing pairs of undistorted lines and undistorted normals. We will see that two distinct ORs arise depending on the chosen pair. If $\boldsymbol{u}$ and $\boldsymbol{h}$ are chosen, the rigid body rotation is calculated to be:

$$\boldsymbol{\gamma R_1 \gamma} = \begin{bmatrix} 0.9911 & -0.0327 & 0.1285 \\ 0.0187 & 0.9939 & 0.1083 \\ -0.1312 & -0.1050 & 0.9857 \end{bmatrix} \tag{5}$$

which is a rotation of 9.8° about $[0.0537\,\overline{0.0654}\,\overline{0.0129}]_\gamma$. The same calculation can be done using $\boldsymbol{u}$ and $\boldsymbol{k}$ and this gives:

$$\boldsymbol{\gamma R_2 \gamma} = \begin{bmatrix} 0.9731 & 0.1050 & 0.2048 \\ -0.0959 & 0.9939 & -0.0537 \\ -0.2092 & 0.0327 & 0.9773 \end{bmatrix} \tag{6}$$

which is a rotation of 13.54° about $[0.0219\,\overline{0.1049}\,\overline{0.0509}]_\gamma$. That is, a distinct rigid body rotation can be obtained with another pair of undistorted lines and undistorted normals. It can be checked that using $\boldsymbol{v}/\boldsymbol{h}$, on the one hand and $\boldsymbol{v}/\boldsymbol{k}$, on the other, leads to rotations that are crystallographically equivalent to those reported for $\boldsymbol{u}/\boldsymbol{k}$ and $\boldsymbol{u}/\boldsymbol{h}$, respectively. Hence, only the solutions involving $\boldsymbol{u}/\boldsymbol{k}$ and $\boldsymbol{u}/\boldsymbol{h}$ will be considered in the following. Then, for the present choice of lattice invariant shear system there exists two different ways for converting the Bain strain into an invariant line strain that read:

$$\boldsymbol{\gamma S_1 \gamma} = \boldsymbol{\gamma R_1 \gamma} * \boldsymbol{\gamma B \gamma} = \begin{bmatrix} 1.1222 & -0.037 & 0.1029 \\ 0.0212 & 1.1253 & 0.0868 \\ -0.1486 & -0.1188 & 0.7892 \end{bmatrix} \tag{7}$$

$$\boldsymbol{\gamma S_2 \gamma} = \boldsymbol{\gamma R_2 \gamma} * \boldsymbol{\gamma B \gamma} = \begin{bmatrix} 1.1018 & 0.1189 & 0.1639 \\ -0.1086 & 1.1253 & -0.043 \\ -0.2369 & 0.037 & 0.7824 \end{bmatrix} \tag{8}$$

Hence, using the same variant of the correspondence matrix, there exist two distinct co-ordinate transformation matrices that read:

$$\boldsymbol{\alpha J_1 \gamma} = \boldsymbol{\alpha C \gamma} * \boldsymbol{\gamma S_1 \gamma}^{-1} = \begin{bmatrix} 0.9042 & -0.8613 & -0.0232 \\ 0.8465 & 0.8944 & -0.2087 \\ 0.1605 & 0.1353 & 1.2313 \end{bmatrix} \tag{9}$$

$$\boldsymbol{\alpha J_2 \gamma} = \boldsymbol{\alpha C \gamma} * \boldsymbol{\gamma S_2 \gamma}^{-1} = \begin{bmatrix} 0.7668 & -0.9627 & -0.2135 \\ 0.9523 & 0.7932 & -0.1559 \\ 0.2559 & -0.0672 & 1.2208 \end{bmatrix} \tag{10}$$

The following relations between planes and direction can be extracted from $\boldsymbol{\alpha J_1 \gamma}$: $(1\,1\,1)_\gamma$ is 0.53° away from $(0\,1\,1)_\alpha$, $[\bar{1}\,1\,0]_\gamma$ is 1.75° away from $[\bar{1}\,0\,0]_\alpha$, $[\bar{1}\,0\,1]_\gamma$ is 3.6° away from $[\overline{1}\,\overline{1}\,1]_\alpha$ and $[1\,1\,\bar{2}]_\gamma$ is 1.67° away from $[0\,1\,\bar{1}]_\alpha$.

This orientation relationship is referred to OR1 and is the one that is usually reported in the experimental observations [6,9–11,15]. It is located midway between KS and NW but closer to NW. It corresponds to a rotation of 44.53° about $[\overline{0.08}\,0.043\,\overline{0.4}]_\gamma$ which can be approximated by $[\bar{2}1\overline{10}]_\gamma$. Similarly, the following relations between planes and directions can be extracted from $\boldsymbol{\alpha J_2 \gamma}$: $(111)_\gamma$ is 0.53° away from $(011)_\alpha$, $[\bar{1}10]_\gamma$ is 8.85° away from $[\bar{1}00]_\alpha$ and $[11\bar{2}]_\gamma$ is 8.86° away from $[01\bar{1}]_\alpha$. This second OR is referred to as OR2. It fulfils the same parallelism condition between compact planes as OR1 (namely $(111)_\gamma//(011)_\alpha$) but compact directions are quite far away from each other. OR2 corresponds to a rotation of 40.96° about $[0.06\,0.09\,0.35]_\gamma$ which can be approximated by $[2311]_\gamma$. The minimum misorientation angle between variants of those two ORs is calculated to be around 7.2°. For each variant of OR1 it is possible to find one, and only one, variant of OR2 which is misoriented from it by a rotation of 60° around a $\langle 111\rangle_\alpha$ direction. That is, variants of OR1 and OR2 can be grouped in pairs that are twin-related. As pointed out by Bowles and Mackenzie, those two solutions have the same shape deformation but differ in the magnitude of the LIS [7]. Indeed, the magnitude of LIS is calculated to be around 0.257 for the solution associated with OR1 while it increases to about 0.4096 for the one associated with OR2. Since the experimental relevance of the low shear solution OR1 has already been assessed, it remains to confirm the prediction of the theory regarding OR2 (high shear solution).

ACOM TEM measurements have been performed on a Fe–30.5Ni–0.155C alloy using the ASTAR® system [17,18]. This alloy is fully austenitic at room temperature (Ms = 220 K) and the martensitic transformation has been induced by cooling in liquid nitrogen. A step size of 4 nm has been used, i.e. ten times smaller than with conventional EBSD. Figure 1a is an ACOM TEM virtual Bright field mapping of two adjoining variants. The corresponding IPF map of the normal direction is reported in Figure 1b.

The transformation twins of the left plate (referred to as α_1 in Figure 1a) are located on only one side of the plate, at the interface between martensite and austenite (γ in Figure 1b). Since the twinned area extends over almost half the thickness of the plate, this transformation product is considered to have been formed at low temperature. This plate α_1 is obviously made up of two orientations referred to as α_1^M and α_1^T in Figure 1b. The average orientations of $\bar{\gamma}$, $\overline{\alpha_1^M}$ and $\overline{\alpha_1^T}$ (calculated using TSL® OIM software) are also reported in Figure 1. The misorientation between $\overline{\alpha_1^M}$ and $\overline{\alpha_1^T}$ is calculated to be close to 60° about $[\bar{1}\,1\,\bar{1}]_\alpha$, thereby confirming that those two orientations are twin-related. The experimental $\{110\}_\alpha$ pole figure of α_1^M (blue points) and α_1^T (red points) projected onto the standard reference frame of austenite is reported in Figure 1c together with the theoretical locations of the $\{110\}_\alpha$ poles of the variants of OR1 (yellow dots) and OR2 (green stars) calculated from the PTMC. This figure clearly shows that α_1^M and α_1^T are very close to OR1 and OR2 predicted from the PTMC, respectively. This observation constitutes the first experimental assessment of the orientation relationship associated with the high shear solution. This orientation relationship would not be expected to be observed on the grounds of strain energy as pointed out by Dunne and Wayman [19], but it is found here as a component of the

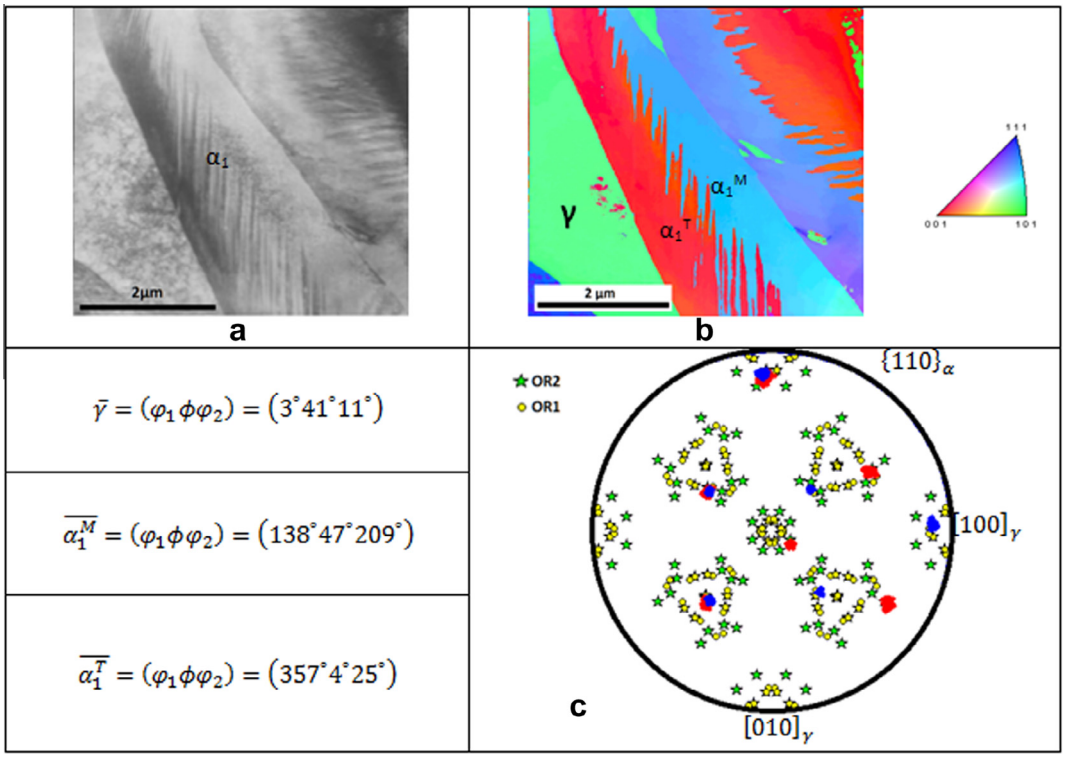

Figure 1. (a) ACOM TEM virtual brightfield image of adjoining variants and (b) corresponding IPF map (c) $\{110\}_\alpha$ pole figure of α_1^M (blue points) and α_1^T (red points) projected in the standard reference frame of their parent austenite (γ in b). (Yellow dot = OR1, Green star = OR2). (For interpretation of color mentioned in this figure legend, the reader is referred to the web version of the article.)

twinned plate of martensite that grows with an overall smaller shape deformation.

It is emphasised, however, that the orientation variant that leads to the high shape deformation has actually never been observed in isolation yet. In this regard, it is worth noticing the unusual disposition of the $\{110\}_\alpha$ poles of the variants of this OR. Indeed, most martensitic transformations in steels produce a typical three fold star pattern in a $\{110\}_\alpha$ pole figure [20,21]. The OR associated with the high shear solution can therefore be distinguished from the classical ORs as it produces tips to this pattern. Two of those tips are indicated by black arrows in Figure 1c. Such an unusual pattern has recently been evidenced by Cayron et al. in the $\{110\}_\alpha$ pole figure of lath martensite formed in a Fe-11.9% Ni-0.04% C-0.32% Si-0.36% Mn-0.15% Cu [21]. Those authors explained this feature by considering that the martensitic transformation occurs in two successive steps. A first γ(fcc)–ε(hcp) transformation followed by a ε(hcp)–α(bcc) transformation. Those tips were believed to be a trace of the rotational part of the deformations associated with those two steps. The present analysis suggests that those tips could also be due to martensite crystals formed directly from the austenite through the high shear path. The fact that this second OR corresponding to a high magnitude of the inhomogeneous shear can form in this alloy can be attributed to its low Ni content. Indeed, Ms is known to increase with a decrease in Ni content [22]. Since the flow stress of austenite decreases with increasing temperature [23], it is believed that the accommodation of this high shear is possible providing a sufficiently high Ms (low Ni content).

In summary, the present study confirms the consistency of the predictions of the phenomenological theory. The two ORs associated with the low and high magnitudes of the LIS hold between the matrix orientation and the austenite and between the twin orientation and the austenite, respectively. The OR associated with the high shear solution implies only the parallelism between the close-packed planes in both phases while close-packed directions deviate from each other by more than 8°. It is suggested that this second OR may hold independently from its twin in lath martensite formed in Fe-low Ni alloys.

[1] K. Shimizu, J. Phys. Soc. Jpn. 17 (1962) 508.
[2] A. Shibata, S. Morito, T. Furuhara, T. Maki, Acta Mater. 57 (2009) 483.
[3] M. Dechamps, L.M. Brown, Acta Metall. 27 (1979) 1281.
[4] R.L. Patterson, C.M. Wayman, Acta Metall. 12 (1964) 1306.
[5] M. Umemoto, K. Minoda, I. Tamura, Metallography 15 (1982) 177.
[6] R.L. Patterson, C.M. Wayman, Acta Metall. 14 (1966) 347.
[7] J.S. Bowles, J.K. Mackenzie, Acta Metall. 2 (1954) 224.
[8] J.S. Bowles, J.K. Mackenzie, Acta Metall. 2 (1954) 129.
[9] A.B. Greninger, A.R. Troiano, Trans. AIME 185 (1948) 590.
[10] A. Shibata, S. Morito, T. Furuhara, T. Maki, Scripta Mater. 53 (2005) 597.
[11] A. Shibata, T. Murakami, S. Morito, T. Furuhara, T. Maki, Mater. Trans. 49 (2008) 1242.
[12] A. Stormvinter, P. Hedström, A. Borgenstam, J. Mater. Sci. Technol. 29 (2013) 373.
[13] H.K.D.H. Bhadeshia, Worked Examples in the Geometry of Crystals, The Institute of Metals, London, 2001.
[14] J.K. Mackenzie, J.S. Bowles, Acta Metall. 2 (1953) 138.
[15] Z. Nishiyama, Martensitic Transformations, Academic Press, New-York, 1978.
[17] E.F. Rauch, L. Dupuy, Arch. Metall. Mater. 50 (2005) 87.
[18] A. Albou, M. Galceran, K. Renard, S. Godet, P.J. Jacques, Scripta Mater. 38 (2013) 400.
[19] D.P. Dunne, C.M. Wayman, Metall. Trans. 2 (1971) 2327.
[20] C. Cayron, Mater. Charact. 94 (2014) 93.
[21] C. Cayron, F. Barcelo, Y. De Carlan, Acta Mater. 58 (2010) 1395.
[22] L. Kaufman, M. Cohen, Prog. Metal Phys. 7 (1958) 165.
[23] R.G. Davies, C.L. Magee, Metall. Trans. 2 (1971) 1939.